

# Safeness Visualization of Terrain for Teleoperation of Mobile Robot Using 3D Environment Map and Dynamic Simulator

Yasuyuki AWASHIMA<sup>1</sup>, Hiromitsu FUJII<sup>1</sup>, Yusuke TAMURA<sup>1</sup>,  
Keiji NAGATANI<sup>1</sup>, Atsushi YAMASHITA<sup>1</sup> and Hajime ASAMA<sup>1</sup>

**Abstract**— In teleoperation of mobile robots on rough terrain, there is a risk that robots might tumble because of the inclination or unevenness of the ground. In this paper, we propose a method to evaluate in advance the stability of robots on assumed routes, and to provide visual information of the stability to the operator. Specifically, by using a 3D environmental map and dynamic simulator, the stability of robots on a terrain with respect to whether the robots are going to tumble or not is calculated. Following this, the information of the stability is visualized as a bird's-eye view image, which is one of the most useful images for the teleoperation of robots. By comparing the results of the actual experiments with those of the dynamic simulator, the validity of the proposed method for the evaluation of stability is demonstrated. The proposed method can help operators to choose suitable routes, and improves the safety in teleoperation of robots.

## I. INTRODUCTION

Quick disaster response is very important for preventing the spread of damage, especially, in the aftermath of earthquakes or floods. In these disaster sites, there may be places that are considered dangerous for humans to enter and act. Therefore, it is highly desirable to use remote controlled robots instead of humans for disaster response [1]–[3]. However, such disaster sites are usually in ruins, and their environments are unknown. The terrain may not be stable enough for robots to move; for example, there could be debris of rocks or fallen trees, and there may be holes or cliffs. In such situations, it is necessary to consider safeness of the terrain in which the robots are operated because the robots cannot return if they crash or tumble due to unstable terrain.

In our previous study [4], we proposed a visualization system that shows the obstacles on the ground surrounding the mobile robot in order to move it safely through disaster sites. This system provides a bird's-eye view of the accurate position of obstacles and virtually views the robot from above by taking three-dimensional measurements of the surroundings of the robot. Although operators can notice obstacles such as fallen trees or lying poles on the ground and can avoid collisions with them using this system, falling or tumbling due to the presence of depressed areas such as holes is inevitable. This is because, the safeness of the terrain, which depends on whether the robot can maintain its stability there, is quite difficult for operators to evaluate using only the visual information.

There have been several studies on the evaluation of safeness of terrain [5]–[8]. Hata *et. al.* proposed methods for the classification of terrain from the perspective of traversability by using terrain features obtained from Laser Range Finder (LRF) measurements [5], [6]. However, the terrain was composed of both good and bad conditions that were apparent (such as pavement and bush), which is quite different from the terrain found in disaster sites. On the other hand, Kondo *et. al.* proposed a path selection method for unmanned ground vehicles running on rough terrain. The study discussed the necessity of considering the physical interaction between the vehicle and terrain [8]. To validate their method, a simulator was developed using a game development system, which included a physics engine and sensor emulators such as LRF, Global Positioning System (GPS) and Inertial Measurement Unit (IMU). Although the study was for the evaluation of terrain traversability based on the results of an actual run using the simulator, the on-site judgment of traversability was done according to the output of a support vector machine that was trained by using just local terrain features. That is, the physical conditions of both the terrain and the vehicle were not considered adequately.

In this paper, a methodology for evaluating the safeness of terrain based on physics simulation using a dynamic simulator, especially a stability criterion, is proposed for the movement of robots through disaster sites. In the proposed method, the local terrain around a robot is measured by using Light Detection and Ranging (LiDAR), and the behavior of a robot moving on the terrain is simulated on site. The safeness of the path to the destination is evaluated for the stability of the robot at the site, and is visualized to help operators decide the direction of movement.

## II. PROPOSED METHOD

### A. Requirements

For the teleoperation of mobile robots, operators need to make decisions on the direction in which robots should proceed on site. However, it is difficult for operators to make accurate judgments in unknown environments. For example, it is difficult to evaluate correctly whether robots can maintain stability during movement due to bad terrain conditions such as holes and cliffs. More specifically, operators cannot obtain adequate information to avoid tumble from only the raw output of sensors such as cameras and LRF. This is because only images can be obtained from cameras, and only 3D points can be obtained from LRF. Thus, to judge whether the direction of movement on is safe for robot teleoperation

<sup>1</sup>Y. Awashima, H. Fujii, Y. Tamura, K. Nagatani, A. Yamashita, H. Asama are with the Department of Precision Engineering, Faculty of Engineering, The University of Tokyo, 7-3-1 Hongo, Bunkyo-ku, Tokyo 113-8656, Japan. {awashima, fujii, tamura, keiji, yamashita, asama}@robot.t.u-tokyo.ac.jp

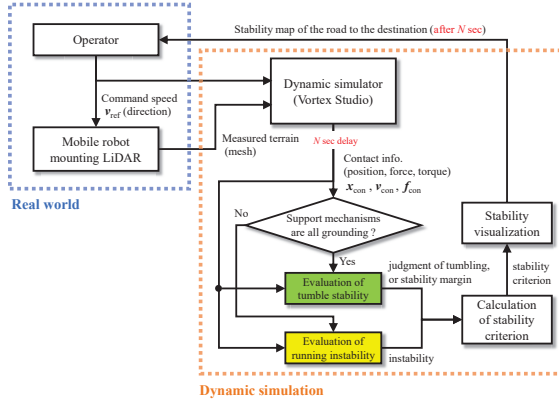


**Fig. 1:** Schematic of the proposed method. The visualized stability of the terrain to the destination is fed back to the teleoperating operator.

in disaster sites, the system must be capable of performing the following tasks:

- 1) Show the stability of the route in a short time.
- 2) Evaluate the stability of the robot on unknown terrain.
- 3) Consider the physical interaction between the terrain and the robot.

### B. System Overview

The schematic of the proposed method is shown in Fig. 1. The system consists of a real part and a simulation part. The input to the dynamic simulator consists of a command velocity from the operator and the 3D environmental map of the terrain obtained by the robot. The environmental map includes the terrain, which is obtained as a point cloud by on-site measurement using a three-dimensional range sensor such as LiDAR. The point cloud is processed into a meshed polygon, which acts as the ground in contact with the robot in the dynamic simulator.

The simulator calculates the contact condition, that is the position, force, and torque of each contact point. In the proposed method, the stability of the robot is evaluated by taking account of the contact state of support mechanisms of the robot. In particular, we newly propose a stability criterion for the safeness estimation of the terrain, and it is visualized as an image that can be viewed by the remote-controlling operators.

### C. Estimation of Stability Criterion

Robots have some kind of support mechanism such as legs or wheels. Several criteria for robotic stability have been proposed [9]–[11]. In these criteria, the robotic stability is based on the tumble stability margin [11]. The tumble stability margin can be used to evaluate the stability of robots by considering the contact points of the support mechanisms with the terrain and the counter force, which varies according to the velocity and acceleration of the robot. Therefore, the tumble stability margin can be suitable for the dynamic movements of robots. However, the tumble stability

margin is not suitable for situations in which any of the support mechanisms is not grounded on the terrain. This is because the tumble stability margin is mainly applicable for movements in which all the support mechanisms are grounded on the terrain.

In actual robot movements, there are supposed to be many situations in which robots do not tumble even if some of the support mechanisms are grounded on the terrain momentarily. Therefore, in this study, robot movements are classified into two: situations in which all the contact mechanisms are grounded and situations in which some are not. Furthermore, let  $S_{SV}$  be the stability value used to evaluate the stability of robots quantitatively.

$$S_{SV} = \begin{cases} S_C & \text{if all contact mechanisms are grounded.} \\ 0 & \text{otherwise} \end{cases}, \quad (1)$$

where  $S_C$  is the value calculated on the basis of the proposed tumble stability margin [11]. The method to calculate  $S_C$  is explained in detail below.

### Tumble Stability Assessment

In this study, the proposed tumble stability margin [11] is used partially for the tumble stability assessment. The details of the proposed tumble stability margin [11] are given below. Let  $\bar{F}$  and  $\bar{M}$  be the force and moment that the entire robot obtains from the ground surface, respectively. The moment  $M_{ab}$  about the line connecting the two contact points  $P_a$  and  $P_b$  can be calculated as follows:

$$M_{ab} = \bar{M} \cdot \frac{\mathbf{p}_a - \mathbf{p}_b}{|\mathbf{p}_a - \mathbf{p}_b|} + \bar{F} \cdot \frac{\mathbf{p}_b \times \mathbf{p}_a}{|\mathbf{p}_a - \mathbf{p}_b|}, \quad (2)$$

where these contact points are not floating up. If there are only two points contacting the ground,  $M_{ab} = 0$  (in eq. (2)) is the condition for the robot to avoid tumbling. In contrast, under the condition  $M_{ab} \neq 0$  the robot tumbles by rotating around the axis  $P_a P_b$ . If there are more than three points contacting the ground the robot does not necessarily tumble, even under the condition  $M_{ab} \neq 0$ . If the direction into which the robot is tumbling corresponds with a direction that presses any other contact points against the ground, the robot is supported by those points and it does not tumble around that axis. Concretely, if a contact point  $P_j$  satisfies the condition

$$\{(\mathbf{p}_j - \mathbf{p}_a) \times \mathbf{n}_j\} \cdot M_{ab} \frac{\mathbf{p}_a \times \mathbf{p}_b}{|\mathbf{p}_a - \mathbf{p}_b|} > 0, \quad (3)$$

the robot is evaluated to not tumble. Here,  $\mathbf{n}_1, \mathbf{n}_1, \dots$  are the normal vectors of each contact point from the ground surface. This evaluation is executed for all combinations of contact points.

If eq. (3) is satisfied for all the contact points around any segment, which includes a combination of two other contact points  $\{P_a, P_b\}$ , the tumble stability margin  $\Delta_+$  can be calculated as a positive value, as shown below.

$$\Delta_+ = \frac{\min \left| \bar{M} \cdot \frac{\mathbf{p}_a - \mathbf{p}_b}{|\mathbf{p}_a - \mathbf{p}_b|} + \bar{F} \cdot \frac{\mathbf{p}_b \times \mathbf{p}_a}{|\mathbf{p}_a - \mathbf{p}_b|} \right|}{mg}, \quad (4)$$

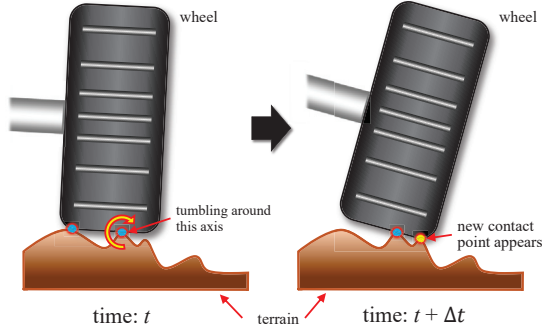


**Fig. 2:** Change of contact points after tumbling. If no contact point satisfies eq. (3) at time  $t$ , the robot is evaluated to be tumbling at the next moment. However, actually the new contact points that can support the robot will be able to appear at time  $t + \Delta t$ . Therefore, the stability of the robot should be evaluated in continuous time.

where  $mg$  is the weight of the robot, and the combination of contact points  $\{P_a, P_b\}$  is restricted to such combinations that meet the condition in which eq. (3) is satisfied for all the contact points except  $\{P_a, P_b\}$ . The above is the detailed description of the tumble stability margin proposed in Ref. [11].

In our proposed method, this tumble stability margin for robots is used as a criterion of the safeness of the path through a if all the support mechanisms of the robot are grounded when it is moving through the terrain. To provide a uniform criterion for the instability status of the robot when any contact dissatisfies eq. (3), we define the stability value  $S_C$  as follows:

$$S_C = \begin{cases} \Delta_+ & \text{if eq. (3) is satisfied for all contacts.} \\ 0 & \text{otherwise} \end{cases} \quad (5)$$

### Definition of Stability Criterion

The contact conditions of the support mechanisms vary during movement on a terrain. For example, when some support mechanisms have no contact with the ground at a particular moment, it should be evaluated as a quite instable condition. However, it is possible that at the next moment all the support mechanisms would be grounded and the robot could return to a stable condition.

Furthermore, even if all the support mechanisms are grounded, and if no contact point satisfies eq. (3) at time  $t$ , the robot is evaluated to tumble at the next moment. However, in reality, the new contact points that can support the robot will be able to appear at time  $t + \Delta t$ , as shown in Fig. 2. Therefore, the stability of the robot should be evaluated in continuous time.

For the above reason, we propose a stability criterion, which considers the continuous change in momentary sta-

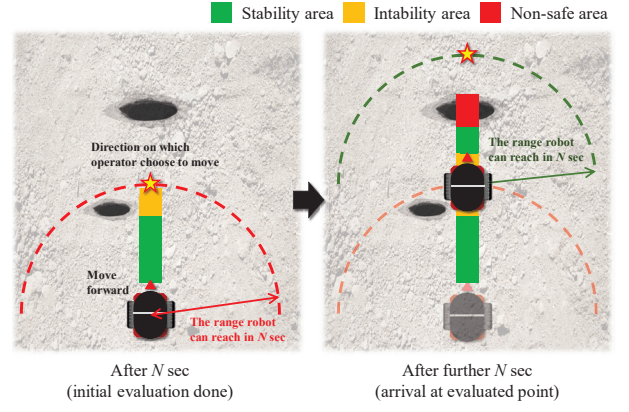


**Fig. 3:** Bird's-eye view of the schematic of the proposed visualization method.

bility. The criterion is evaluated once every unit time.

$$\text{Stability} = \begin{cases} \text{Tumble, if } S_{SV} \text{ is 0 during the entire unit time.} \\ \text{Instable, else if } S_{SV} < \theta \text{ during over a half of} \\ \text{the unit time.} \\ \text{Stable, otherwise.} \end{cases} \quad (6)$$

where  $\theta$  is a threshold that should be determined by referring a stability value  $S_{SV}$  of the movement through a safe environment such as a flat terrain, for example it can be set as half of the stable value.

### D. Stability Visualization

It has been validated in many researches and applications that the bird's-eye view is appropriate for robotic teleoperation, especially for movement [4], [12]–[15]. That is the reason why, in the proposed method, the stability of the path to the destination is visualized as a bird's-eye view, as shown in Fig. 3.

Before a robot moves, the left figure in Fig. 3 is presented to its operator. By using this figure, the operator first chooses the destination from the reachable points, which are indicated by the red semicircle in the figure, in  $N$  seconds. After the calculation time of  $N$  seconds, the operator can check the stability of the robot on the path to the destination, which is shown as a thick line segment in green, yellow, or red in this figure. If the path is safe, the operator actually moves the robot to the destination. On the simulator, the stability of the robot is continued to be calculated under the assumption that the robot maintains the same forward movement towards the destination while is in motion to the destination. When the robot reaches the destination, the image shown in the right figure of Fig. 3 is presented to the operator. Using this image, the operator can check the stability of the robot on the path beyond the first destination, for a distance that be move by the robot in an additional  $N$  seconds. This is because the stability of the robot on this path is calculated while the

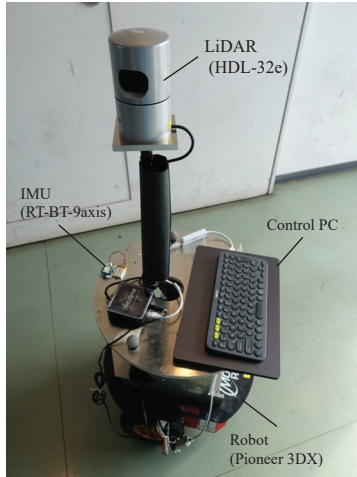


**Fig. 4:** Robot used in the experiment: Pioneer 3DX with a mounted LiDAR HDL-32e.

robot is moving to the first destination, as mentioned above. Thus, if the robot can keep on moving in the same direction, the image in which the stability of the robot is visualized can be continuously presented to the operator.

Using this stability visualization, the operator can check the stability of the robot from the images with few calculation delays and high visibility provided by the of bird's-eye view.

### III. EXPERIMENTS

#### A. Visualization System with Simulator

In order to verify our system for tumble avoidance, experiments were performed using a mobile robot that was controlled remotely. In this section, the remote control system for assessing the safeness of the terrain surrounding the robot in disaster sites, considering the stability of the robot during movement, is described.

#### Dynamic Simulator:

The dynamic simulator shown in Fig. 1, which is based on Vortex Studio [16] by CM Labs Simulations, is equipped with a real-time physics engine. The physics engine can conduct real-time simulation of the multibody dynamics, including the calculation of the contacts between the robots and other objects such as the ground. The simulator outputs physical information such as the poses of the robot parts (the body or the wheels) and their contact forces/torques for every 16 ms, and the proposed method can be used to evaluate the stability of the robot at those moments.

With regard to physical simulation, the physical parameters of the ground were set heuristically so that the contact between the wheels of the robot and the ground can be simulated adequately.

#### Mobile Robot with LiDAR:

In the proposed system, the robot measures the three-dimensional terrain of the surrounding environment during movement. The robot system constructed for the experiments

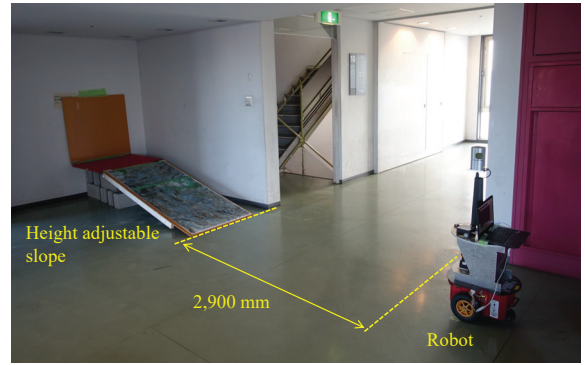


**Fig. 5:** Experimental environment: There is a slope-shaped apparatus whose angle can be adjusted. The robot scanned the environment at the position shown in this figure (at a distance of about 3,000 mm from the slope), and evaluated the safeness of the terrain.

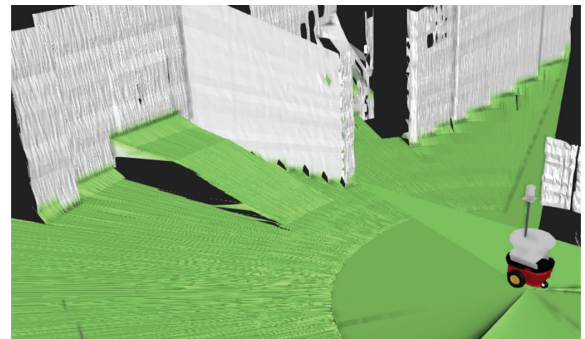


**Fig. 6:** A scene from the proposed simulator using Vortex Studio, which includes a physics engine. The physical properties of the robot such as the center of mass and inertia were set that it accurately simulates the behavior of the robot on the measured terrain.

is shown in Fig. 4. Pioneer 3DX from MobileRobots Inc. was used as the mobile robotic platform. In order to measure the surrounding environment and obtain the mesh model of the terrain, HDL-32e from Velodyne LiDAR Inc. was installed on the robot. This LiDAR sensor can obtain three-dimensional information, or distances from objects in the surrounding environment for a range of 1 m to 100 m by irradiating 32 laser lines. This sensor is adequate for outdoor usage, because its principle of measurement is Time of Flight using laser beams that are robust against the influence of infrared rays from sunlight. Furthermore, in order to obtain the gradient of the terrain in the world coordinate system, a Bluetooth IMU (RT-BT-9axisIMU of RT Corp.) was mounted on the robot.

For accurate simulation, the physical properties of the robot, such as the precise shape of the parts and the center of mass are necessary. For this experiment, 3D CAD models of the robot and the jig for fixing the sensors were prepared, and the center of mass was measured by using a force plate TF-4060 (Tech Gihan Co., Ltd.).

TABLE I: Experimental settings of slopes

Slope type	Height [mm]	Inclination angle [deg]	Result of actual experiment
Steep-inclined	480	15.4	Up: <b>Tumble</b>
Moderate-inclined	380	12.2	Up: <i>Stable</i> / Down: <b>Tumble</b> (forward), <i>Unstable</i> (backward)
Gentle-inclined	290	9.2	Up: <i>Stable</i> / Down: <i>Stable</i>

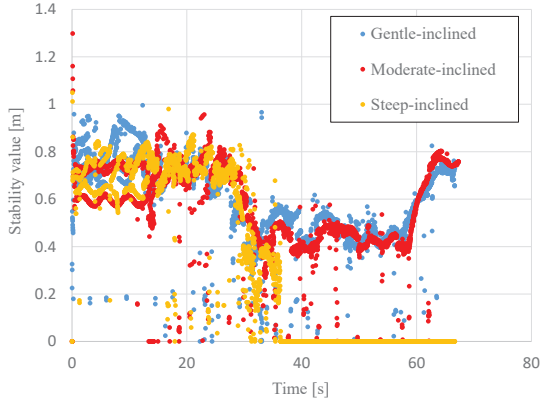


Fig. 7: Stability value when the mobile robot moved up each type of slope on the simulator. The mobile robot moved on a flat floor for about 30 s before climbing each type of slope.

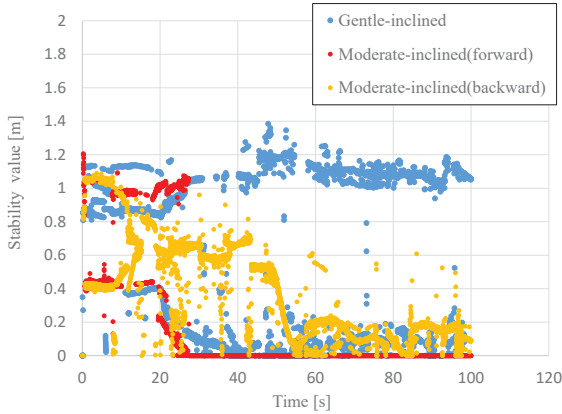
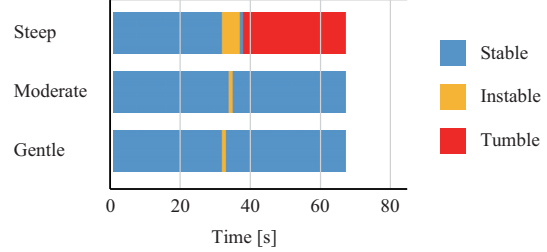


Fig. 8: Stability value when the mobile robot moved down each type of slope on the simulator. The mobile robot moved on a flat terrain for about 10 s before descending each type of slope.

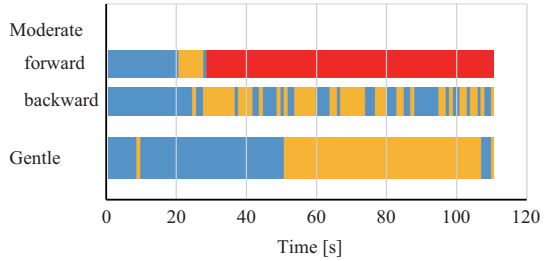
### B. Environmental Settings

In order to validate the proposed method, a slope-shaped apparatus, whose angle can be adjusted, was set in an indoor hall, as shown in Fig. 5. The experimental environment was a terrain having slopes with different angles of inclination and heights. Three types of slopes were prepared, as shown in Table I. The robot climbed up to the top of the slope and then returned.

With regard to the environmental measurement, the robot scanned the surrounding environment using LiDAR at a distance of about 3,000 mm from the slope; the position



(a) Stability criterion for climbing up each type of slope on the simulator. In regard to the steep-inclined slope, the stability criterion showed that the robot would tumble



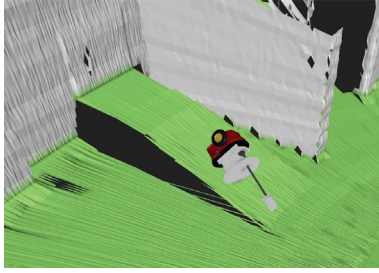
(b) Stability criterion for descending each type of slope on the simulator. In regard to the steep-inclined slope, the stability criterion was not calculated because the robot could not climb up the steep-inclined slope. Furthermore, in regard to the moderate-inclined slope, the stability criterion showed that the robot would tumble when the robot's orientation was forward. Therefore, in addition to this, the stability criterion when the robot's orientation was backward was calculated.

Fig. 9: Stability criterion.

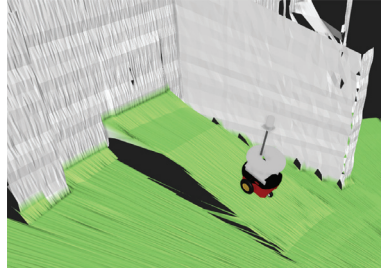
is shown in Fig. 5. The terrain scanned by the LiDAR was input into the system on site, and the physical behavior of the robot was calculated in real time. The experimental scene in the simulator corresponding to the scene in Fig. 5 is shown in Fig. 6. In this experiment, the 3D environmental map obtained by the LiDAR was loaded only once; however the 3D environmental maps need to be reloaded at least each time the robot moves about 100,000 mm, because of the limited measurement range of the LiDAR.

The command velocity was set to be slow enough for careful movement, about 40 mm/s while climbing up, and about 20 mm/s while climbing down. In the simulation, the robot was controlled using a joystick so that the operators can easily change the command velocity and direction as necessary.

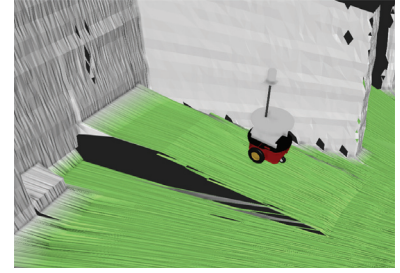
The unit time used for evaluating the stability criterion was about 60, and the delay time  $N$  was about 20. These values were determined by taking the command velocity and



(a) Tumbling on the steep-inclined slope.  
(480 mm height, 15.4 deg angle)



(b) Instable movement on the moderate-inclined slope.  
(380 mm height, 12.2 deg angle)



(c) Stable movement on the gentle slope.  
(290 mm height, 9.2 deg angle)

**Fig. 10:** Simulation results: (a) The system evaluated that the robot could not climb up the steep-inclined slope in stable condition. (b) The result showed that the robot could climb up the slope with slight instability. However, while descending, the robot could not move forward with stability, and therefore it had to return with backward movement.



(a) Steep-inclined slope



(b) Moderate-inclined slope



(c) Gentle-inclined slope

**Fig. 11:** Experiments using three types of terrain. Each terrain has a slope whose height is different each other.

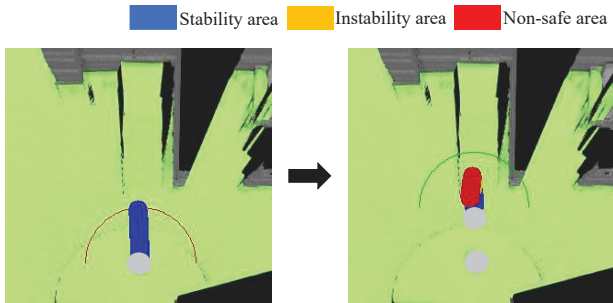


**Fig. 12:** Visualization result of the safeness of the path to the destination.

the appearance of the terrain into account. Therefore, these values can be changed depending on these factors.

### C. Results

Figure 7 shows the stability value when the mobile robot moved up each type of slope on the simulator. The mobile robot moved on the flat floor for about 30 s before climbing each type of slope. In this figure, the blue dots, red dots, and

yellow dots indicate the stability value when the mobile robot moved up the gentle-inclined slope, moderate-inclined slope, and steep-inclined slope, respectively. Figure 8 shows the stability value when the mobile robot moved down each type of slope on the simulator. The mobile robot moved on a flat terrain for about 10 s before descending each type of slope. In this figure, the blue dots indicates the stability value when the mobile robot moved down the gentle-inclined slope. The red and yellow dots indicate the stability value when the mobile robot moved down the moderate-inclined slope forward and backward, respectively. In Figs. 7 and 8, the dots whose stability value is zero indicate cases in which no contact point satisfies eq. (3) or any of the support mechanisms was not grounded on the terrain in the moment. From Figs. 7 and 8, it can be seen that the stability value tended to decrease when the mobile robot was moving on each slope. Thus, the results shown in Figs. 7 and 8 clearly illustrate the instability of the robot on each type of slope.

Figs. 9 (a) and (b) show the final evaluation of stability using the stability margin as the proposed stability criterion. Fig. 9 (a) shows the final evaluation of stability when the mobile robot climbed up each slope, and Fig. 9 (b) shows the final evaluation of stability when the mobile robot moved

down each slope. In Fig. 9, the blue, yellow, and red colors indicate the duration for which the mobile robot was stable, instable and, tumbling, respectively. In relation to Figs. 9 (a) and (b), the actual appearances of the simulation are shown in Fig. 10. From Figs. 9 (a) and (b), it can be seen that the final evaluations of stability are consistent with the experimental results obtained by using the actual mobile robot, which is shown in TABLE I.

The results of the experiments using the actual robot are shown in Fig. 11, and an example of the visualized stability during the movement shown in Fig. 10 (a), which is explained in Section II-D, is shown in Fig. 12. By using the images of Fig. 12, operators could select the suitable routes, and were successful in teleoperating the robot safely. In particular, in the experiment shown in Fig. 11 (b), the robot could return safely by descending backward.

#### IV. CONCLUSIONS

In regard to disaster response using remote controlled robots, we proposed a method for evaluating the safeness of the terrain surrounding a robot. The constructed system consists of a mobile robot mounting a LiDAR for three-dimensional measurement of the environment and a dynamic simulator for considering the interaction between the robot and terrain. In the proposed method, the safeness of terrain is evaluated in terms of the stability of the robot during the movement.

In our experiments, the validity of the proposed method was confirmed through actual robot movements, which were similar to the simulation output. The system accurately evaluated the safeness of the routes.

Examples of representative robots working in disaster sites are construction equipment such as excavators. In our future work, we will apply this system to construction equipment for unmanned construction.

#### ACKNOWLEDGMENTS

This work was in part funded by ImPACT Program of Council for Science, Technology and Innovation (Cabinet Office, Government of Japan). The authors also would like to thank the members of Intelligent Construction Systems Laboratory, the University of Tokyo, for useful suggestions, especially Mr. Shingo Yamamoto and Mr. Takumi Chiba from Fujita Corporation and Dr. Kazuhiro Chayama from KOKANKYO Engineering Corporation.

#### REFERENCES

- [1] F. Matsuno and S. Tadokoro: "Rescue Robots and Systems in Japan," Proceedings of the 2004 IEEE International Conference on Robotics and Biomimetics, pp. 12–20, 2004.
- [2] M. W. Kadous, R. K. Sheh and C. Sammut: "Effective User Interface Design for Rescue Robotics," Proceedings of the 1st ACM SIGCHI/SIGART Conference on Human-Robot Interaction, pp. 250–257, 2006.
- [3] K. Chayama, A. Fujioka, K. Kawashima, H. Yamamoto, Y. Nitta, C. Ueki, A. Yamashita and H. Asama: "Technology of unmanned construction system in Japan," Journal of Robotics and Mechatronics, vol. 26, no. 4, pp. 403–417, 2014.
- [4] Y. Awashima, R. Komatsu, H. Fujii, Y. Tamura, A. Yamashita and H. Asama: "Visualization of Obstacles on Bird's-eye View Using Depth Sensor for Remote Controlled Robot," Proceedings of the 2017 International Workshop on Advanced Image Technology, 2017.
- [5] A. Y. Hata and D. F. Wolf: "Terrain mapping and classification using Support Vector Machines," Proceedings of the 2009 6th Latin American Robotics Symposium, pp. 1–6, 2009.
- [6] A. Y. Hata, D. F. Wolf, G. Pessin and F. Osorio: "Terrain Mapping and Classification in Outdoor Environments Using Neural Networks," International Journal of u-and e-Service, Science and Technology, vol. 2, no. 4, pp. 51–61, 2009.
- [7] Y. Tanaka, Y. Ji, A. Yamashita and H. Asama: "Fuzzy Based Traversability Analysis for a Mobile Robot on Rough Terrain," Proceedings of the 2015 IEEE International Conference on Robotics and Automation, pp. 3965–3970, 2015.
- [8] M. Kondo, K. Sunaga, Y. Kobayashi, T. Kaneko, Y. Hiramatsu, H. Fujii and T. Kamiya: "Path Selection Based on Local Terrain Feature for Unmanned Ground Vehicle in Unknown Rough Terrain Environment," Proceedings of the 2013 IEEE International Conference on Robotics and Biomimetics, pp. 1977–1982, 2013.
- [9] E. Garcia, J. Estremera and P. Gonzalez-de-Santos: "A Classification of Stability Margins for Walking Robots," Proceedings of the 2002 International Symposium on Climbing and Walking Robots, vol. 2002.
- [10] E. Garcia, J. Estremera and P. Gonzalez-de-Santos: "A Comparative Study of Stability Margins for Walking Machines," Robotica vol. 20, no. 6, pp. 595–606, 2002.
- [11] K. Yoneda and S. Hirose: "Tumble stability criterion of integrated locomotion and manipulation," Proceedings of the 2006 IEEE/RSJ International Conference on Intelligent Robots and Systems, vol.2, pp. 870–876, 1996.
- [12] Y. C. Liu, K. Y. Lin and Y. S. Chen: "Bird's-eye View Vision System for Vehicle Surrounding Monitoring," Proceedings of the 2008 International Workshop on Robot Vision, pp. 207–218, 2008.
- [13] C. C. Lin and M. S. Wang: "Topview Transform Model for The Vehicle Parking Assistance System," Proceedings of the 2010 International Computer Symposium, pp. 306–311, 2010.
- [14] S. Shimizu, J. Kawai and H. Yamada: "Wraparound View System for Motor Vehicles," Fujitsu Scientific & Technical Journal, vol. 1, no. 46, pp. 95–102, 2010.
- [15] J. Mingyue, Y. Sun and J. Wang: "Obstacle Detection in Stereo Bird's Eye View Images," Proceedings of the 2014 Information Technology and Artificial Intelligence Conference, pp. 254–257, 2014.
- [16] "Theory Guide: Vortex Studio's Multibody Dynamics Engine," CM Labs Simulations, <https://www.cm-labs.com/>.